Experimental and theoretical approach to evaluation of nanostructured carbon particles derived from phenolic resin via spray pyrolysis

Aditya F. Arif, Ratna Balgis, Takashi Ogi, Takahiro Mori, Kikuo Okuyama

PII: S1385-8947(15)00287-9
DOI: http://dx.doi.org/10.1016/j.cej.2015.02.078
Reference: CEJ 13331

To appear in: *Chemical Engineering Journal*

Received Date: 27 December 2014
Revised Date: 17 February 2015
Accepted Date: 23 February 2015

Please cite this article as: A.F. Arif, R. Balgis, T. Ogi, T. Mori, K. Okuyama, Experimental and theoretical approach to evaluation of nanostructured carbon particles derived from phenolic resin via spray pyrolysis, *Chemical Engineering Journal* (2015), doi: http://dx.doi.org/10.1016/j.cej.2015.02.078

Experimental and Theoretical Approach to Evaluation of Nanostructured Carbon Particles Derived from Phenolic Resin via Spray Pyrolysis

Aditya F. Arif[a], Ratna Balgis[a*], Takashi Ogi[a], Takahiro Mori[a], Kikuo Okuyama[a]

[a]Department of Chemical Engineering, Graduate School of Engineering, Hiroshima University
1-4-1 Kagamiyama, Higashi-Hiroshima 739-8527, Japan

*Corresponding Author. Tel: +81-82-424-7850. Fax: +81-82-424-7850.
E-mail: ratna-balgis@hiroshima-u.ac.jp

Abstract

Dense and porous nanostructured carbon particles were successfully synthesized via spray pyrolysis of phenolic resin and polystyrene latex. An approach to estimate the size and size-distribution of the synthesized carbon particles is presented here. The size of dense carbon particles was found to be mainly determined by the concentration of phenolic resin in the precursor. Meanwhile, the size and morphology of porous carbon particles were found to be affected by the concentration of the polystyrene latex particles used as the template. A residual ratio was introduced as a variable to represent the shrinkage due to phenolic resin decomposition. New correlations were developed that permit estimation of the mean diameter and size-distribution of the synthesized carbon particles from the phenolic resin concentration. Good agreement was observed between predicted values and experimental results.

Keywords: Particle size, Size-distribution, Nanostructurization, Carbon particle, Sprayed droplets, Morphology

1. Introduction

The aerosol process allows scalable synthesis of functionalized, ultrafine particles with particular physical and chemical properties from molecular precursors [1, 2]. In this method, particles are produced by either a droplet-to-particle or a gas-to-particle conversion process [3]. Spray drying is one of the droplet-to-particle methods for a wide range of applications, e.g. pharmaceuticals, foods, ceramics or catalysts [4-6]. Here, structured particles are produced from a particle suspension or a colloidal mixture that is atomized to form ultrafine droplets whose volumes are mostly occupied by solvent. The solvent is then evaporated by heating, causing the remaining components to precipitate after the mixture reaches a super-saturated state. This whole process can be carried out in several seconds [7]. The produced particles may exhibit a range of sizes and morphologies according to the characteristics of precursor, the size of the droplets and other operating conditions. Particles with a narrow size-distribution are preferable to obtain homogeneous properties, for example for understanding flow and dispersion [6, 8, 9]. In light of this preference, ultrasonic atomization—rather than two-phase atomization—tends to be used for droplet production since it can produce tightly-controlled, micrometer-sized droplets [10].

Ultrafine particles with a narrow size-distribution and controllable morphology can also be synthesized by spray pyrolysis. Although the basic principle is similar to that for spray drying, the presence of chemical decomposition at elevated temperatures differentiates spray pyrolysis [11], as shown in Figure 1. The precursor of the spray pyrolysis process is usually metal salts or simple organic materials [12]. For example, phenolic resin was successfully used as the starting material for carbon particle synthesis by pyrolysis [13-16], and also has potential for scaled-up carbon particle production as it is a relatively low-cost raw material.

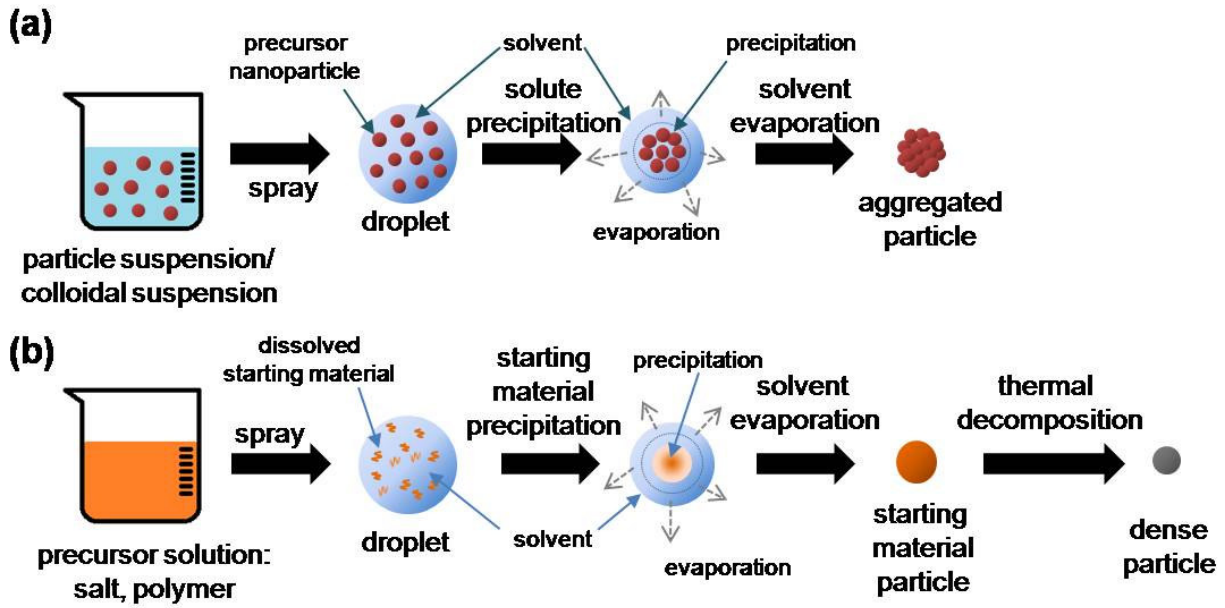

Figure 1.Illustration of spray drying (a) and spray pyrolysis (b)

In the scaled-up production of nanostructured carbon particles, the particle surface area is a key quality objective. For example, for particles used as catalysts a higher surface area is desired because it is one of the factors that determine catalytic activity. Because particle size and morphological structure are among the determining factors of particle surface area, a number of works have studied these factors. Morphological control of carbon particles, including control of the pore size and structure, has been carried out using a number of techniques, such as employing a template and using different derivations of phenolic resin [17, 18]. Controlling the particle size requires an adequate understanding of the factors that contribute to the particle size and the correlation between them. Through such correlation, the concentration of phenolic resin that is required to attain certain particle size can be determined.

Correlation between the final particle size and the starting material in the case of spray drying has been studied with the particle size found to be predicted by the following equation [19, 20].

$$D_{p,v} = D_{d,v}\left(\sum_{i=1}^{n}\frac{C_i M_i}{\rho}\right)^{1/3} \quad (1)$$

$D_{p,v}$, $D_{d,v}$, C, M, ρ denote the average particle diameter, the average droplet diameter, the droplet concentration, the molecular weight of droplet and the particle mass density, respectively. The subscript i corresponds to the component sequence. Although some disagreements were reported at certain levels of starting material concentration [19], most of experimental data for both dense and porous particles showed good agreement with the correlation in terms of particle size and particle size distribution [7, 20].

Although Equation (1) demonstrates the correlation for spray drying, to the best of our knowledge a correlation between particle size and precursor properties specifically applicable to nanostructured carbon particle synthesis by spray pyrolysis has not yet been developed. Indeed, Equation (1) may not be applicable for carbon particles derived from phenolic resin using spray pyrolysis because the equation only considers water evaporation during particle generation. However, in the spray pyrolysis of phenolic resin, several gases are also released through polymeric reactions which have important implications for predicting particle size [21]. Notably, the loss of these gases will decrease the mass of the synthesized particles, causing the particle to shrink after carbonization. Understanding the decomposition stoichiometry is one approach to evaluate the particle size but this is difficult for the phenolic resin decomposition where the stoichiometry is difficult to determine. Therefore, another approach is needed toevaluate the carbon particle size.

This paper aims to define an approach to establish new correlations to estimate the size and size-distribution of dense and porous carbon particles formed by spray pyrolysis. The correlations include a parameter to represent phenolic resin decomposition in spray pyrolysis and pores formation due to the addition of a template molecule.

2. Material and Methods

2.1. Carbon particle synthesis

Two types of carbon particles—dense and porous—were prepared. Dense carbon particles were prepared from an aqueous solution containing resole-type phenolic resin (Sumitomo Bakelite Co., Ltd., Tokyo, Japan) as the precursor. Five concentrations of the phenolic resin were used; 0.06, 0.125, 0.25, 0.5 and 1 wt%. A mixture of phenolic resin and negatively-charged polystyrene latex (PSL; particle size of ~230 nm) was prepared for porous

carbon particle production. The phenolic resin concentration was maintained at 0.25 wt% while the mass ratio of PSL to phenolic resin was studied at 0.8, 1.6 and 3.2.

Spray pyrolysis experiments were carried out using the setup shown in Figure 2. The apparatus consists of an ultrasonic nebulizer (1.7 MHz, NE-U17, Omron Healthcare Co., Ltd., Kyoto, Japan) for droplet production, a tubular furnace (length: 1100 mm; inner diameter: 13 mm) and a filter where sample was collected. The furnace was divided into low- and high-temperature zones, with each zone including two sections. The upper and lower sections in the low-temperature zone were maintained at a temperature of 350 and 150 °C, respectively. The temperature in the high-temperature zone was determined following the preliminary experiments detailed below. Nitrogen (N_2), flowing at 0.8 L min^{-1}, was used as the inert carrier gas.

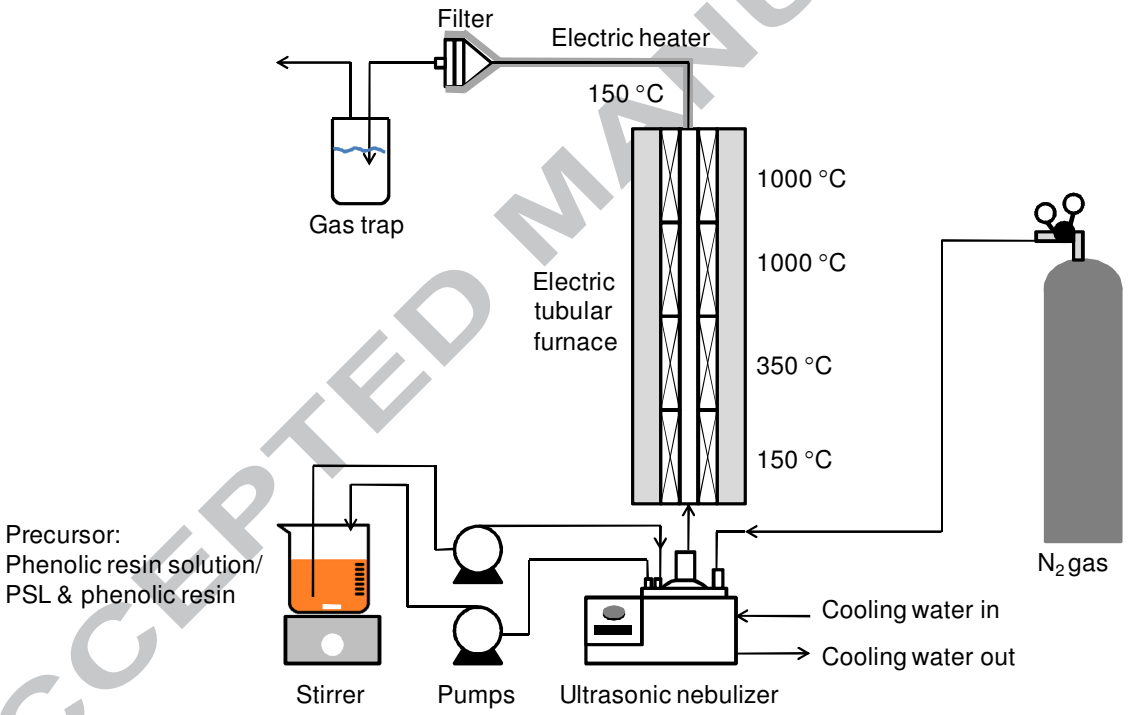

Figure 2. Schematic of spray pyrolysis experiment

2.1.1. Preliminary experiments

Preliminary experiments were carried out to determine the optimum temperature configuration for the high-temperature zone. According to thermogravimetric analysis of phenolic resin decomposition in an inert environment [22], water evolution from condensation reactions start when temperatures increase above 350 °C. Methylene scission leading to drastic

decomposition then occurs at approximately 500°C. At a temperature of 800 °C the weight-loss curve showed relatively small changes, indicating that carbonization nears completion at this temperature [23]. Further analysis with the furnace shown in Figure 2 operating at different temperatures resulted in the various particles presented in Figure 3. After spray pyrolysis at 350 °C, yellow-colored particles were obtained with no major decomposition assuming to have taken place (Figure 3a). Spray pyrolysis at 500 °C resulted in the brown-colored particles (Figure 3b) confirming the onset of significant decomposition. At 850 °C, black-colored particles were obtained, as shown in Figure 3(c), indicating that the carbonization process was almost complete. Figure 3(d) also shows black particles, which resulted from temperatures of 1000 °C. Considering the short residence time during spray pyrolysis, the potential for a non-uniform temperature distribution and some, albeit small, changes in the weight-loss curve at 800 °C, it was decided to perform spray pyrolysis at the higher temperature of 1000 °C.

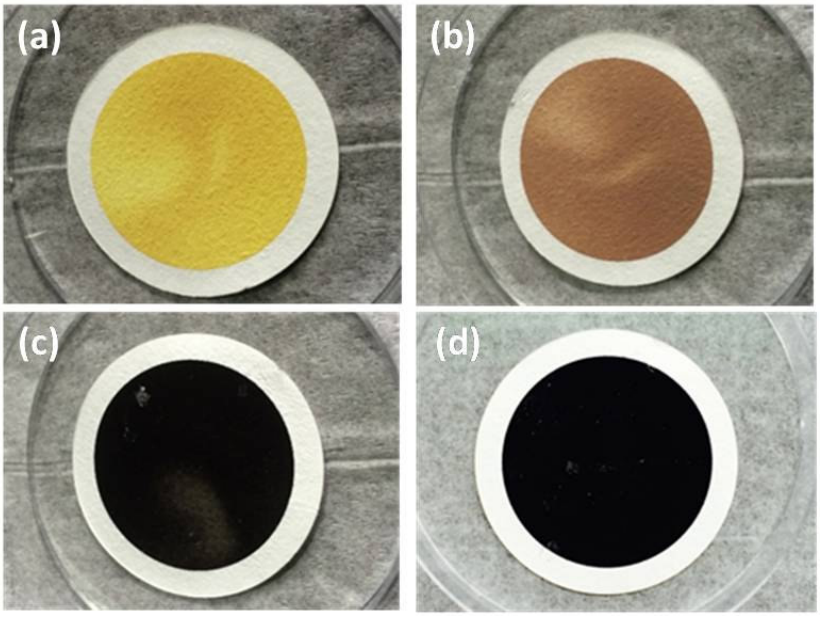

Figure 3. Color of captured material prepared at (a) 350 ºC, (b) 500 ºC, (c) 850 ºC and (d) 1000 °C.

The temperature distribution inside the furnace was then modeled using a heat transfer simulation (Flex PDE 6.0) using the following equation.

$$\rho C_p v_z \left(\frac{\partial T}{\partial r}\right) = k\left(\frac{\partial^2 T}{\partial r^2}\right) \qquad (3)$$

z and r are the axial and radial directions, respectively. Figure 4 shows the furnace temperature distribution for temperatures of 150 and 350 °C for the low-temperature zone, and 1000 °C for the high-temperature zone. At the N_2 flowrate of 0.8 L min^{-1}, the heating rates of zone I, zone II, and the combination of zones III and IV, was estimated to be 45, 50 and 145 °C s^{-1} respectively. These values for heating rate and temperature distribution were considered acceptable for performing spray pyrolysis.

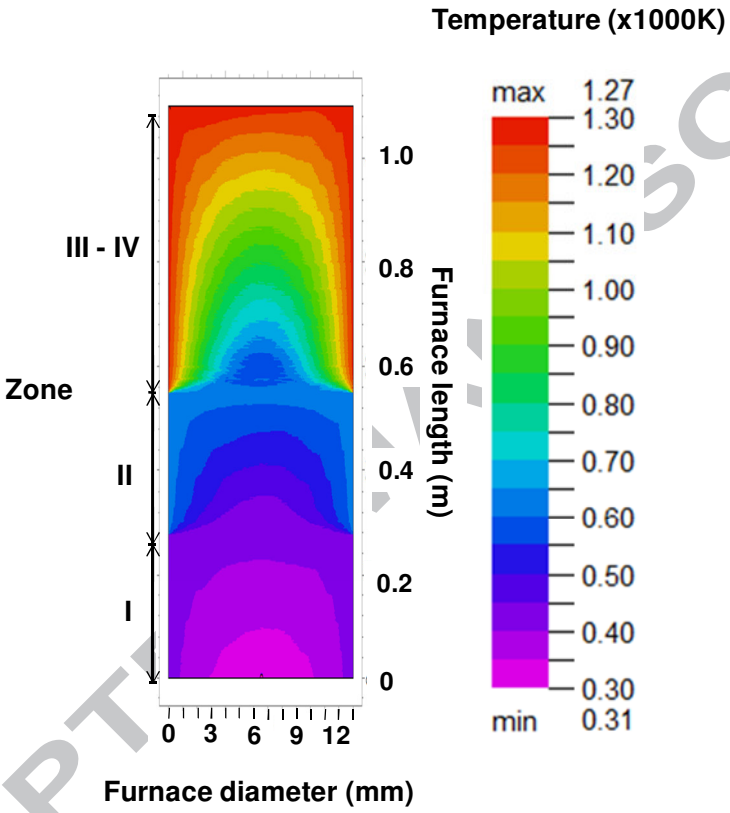

Figure 4. Furnace temperature distribution

2.2. Droplet characterization

Droplet diameter was measured using the laser diffraction technique (Spraytec, Malvern Instrument Ltd., Malvern, UK) while the surface tension of the precursor solutions was measured using a Wilhelmy Plate Tensiometer (Kyowa Interface Science Co. Ltd., Saitama, Japan).

2.3. Particle characterization

The physical morphology of the particles was observed using a field-emission scanning electron microscope (SEM; S-5000, 20kV, Hitachi High-Tech. Corp., Tokyo, Japan), while the porosity of the particle was estimated using topological observation. Number-average particle

diameters ($D_{p,n}$) were determined by measuring the diameter of more than 300 randomly-selected particles. The obtained $D_{p,n}$ were then converted to volume-average diameters ($D_{p,v}$) using Equation (2).

$$D_{p,v} = \left[\sum \left(\frac{\Delta N D_{p,n}^3}{N} \right) \right]^{1/3} \quad (2)$$

All of the experiments, including spray pyrolysis, droplet characterization and particle characterization, were conducted three times. Average value was taken from three separate sets of data.

3. Results and Discussion

3.1. Morphological structure

After spray pyrolysis at 1000 °C, spherical dense particles were obtained from the phenolic resin precursor, as shown in the single-particle SEM images in Figure 5. Che et al. [24] and Lenggoro et al. [25] stated that dense particles could be formed if simultaneous precipitation took place within the droplet, with this process dependent on the solute concentration profile inside the droplet [26]. The concentration profile of the phenolic resin depends on the diffusion rate of phenolic resin within the droplet and rate at which water evaporates. Taking these two parameters into consideration, we hypothesize that simultaneous precipitation in the spray pyrolysis of phenolic resin-water system occurs due to the very rapid diffusion of phenolic resin within the droplet relative to the water evaporation rate. Rapid diffusion of the phenolic resin allows faster self-assembly, which results in the higher phenolic resin concentration at the center of the droplet (negative concentration gradient). Rapid phenolic resin diffusion may be attributed to the low heating rate in the water evaporation stage [25].

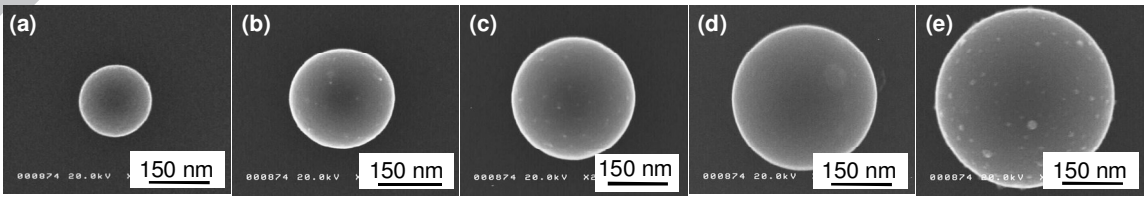

Figure 5. SEM images of single, dense particles generated from phenolic resin at a concentration (wt%) of (a) 0.06, (b) 0.125, (c) 0.25, (d) 0.5, and (e) 1.0.

According to Figure 5, all of the obtained particles were completely spherical with no trace of particle explosion. Particle explosion usually occurs due to a pressure build up inside the crust [27], with the crust formed when the solute at the droplet surface reaches its super-saturation state. The absence of a crust in these images supports the hypothesis that the self-assembly process of phenolic resin was more rapid than the water evaporation rate.

At similar operating conditions, the addition of negatively-charged PSL particles allows the formation of pores, as seen in Figure 6. Here, both phenolic resin and PSL self-assembled within the droplet. Because both phenolic resin and PSL were negatively charged, phenolic resin and PSL particles repelled each other causing both sets of particles to be independently distributed throughout the droplet. When exposed to high temperatures the PSL particles decomposed leaving pores in the structure. As the concentration ratio of PSL to phenol resin was increased, PSL particles occupied a greater proportion of the droplet with their decomposition giving rise to a synthesized carbon with a higher porosity, as shown in Figure 6.

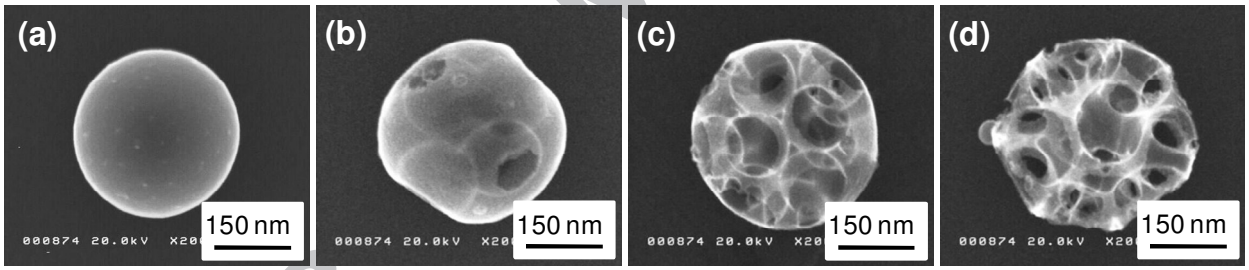

Figure 6. SEM images of single, porous particles produced from PSL: phenolic resin precursor mixtures of (a) 0, (b) 0.8, (c) 1.6 and (d) 3.2. For all cases the phenolic resin concentration was 0.25 wt%

3.2. Trends of final particle size

3.2.1. Dense particles

Figure 7 shows the increase in particle size with increasing concentration of phenolic resin. This result aligns with the trend predicted by Equation (1) despite the significant deviation in the predicted particle size. Because the phenolic resin was homogeneously mixed, a uniform phenolic resin concentration can be assumed across the droplets. At higher concentrations of phenolic resin, more phenolic resin was available in the droplet to precipitate during the spray

pyrolysis. Particle formation was assumed to follow the one-droplet-one-particle principle. Therefore, higher phenolic resin concentration is expected to result in large particles.

However, Figure 8 (a) shows that the trend in the droplet size is inversely proportional to the trend of the particle size. This is likely explained by the fact that the addition of phenolic resin acts to decrease the surface tension. Here, according to the correlations proposed by Lang et al. [28] and Rajan et al. [10], a decrease in surface tension leads to a decrease in the size of the droplets produced by the ultrasonic nebulizer, as shown in Figure 8 (b). Nevertheless, the experimentally-derived relationship between the droplet and particle diameters seems to disagree with Equation (1), in which particle diameter is proportional to both droplet diameter and phenolic resin concentration. This disagreement emphasizes that the concentration of the solute is more important than the droplet size in determining the final particle diameter.

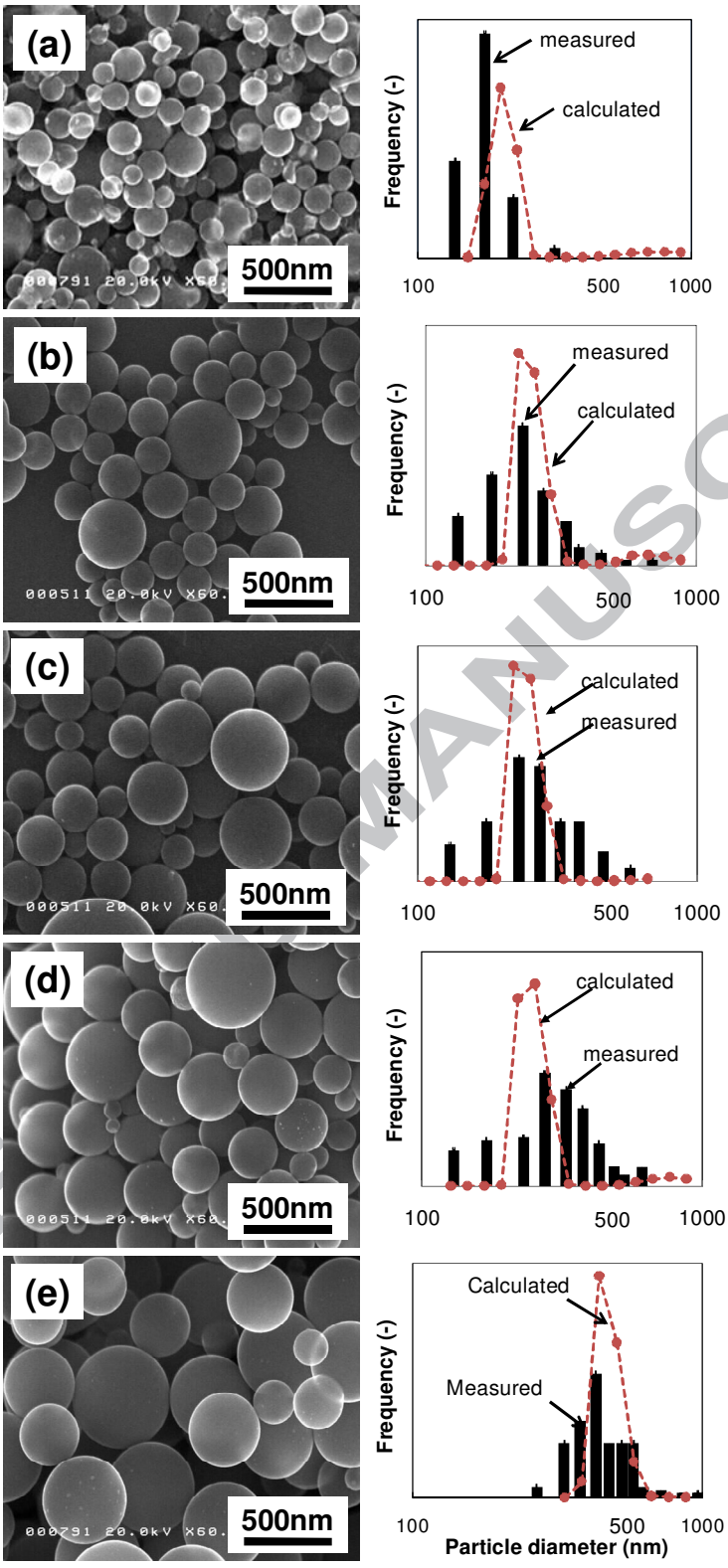

Figure 7. SEM images and size-distributions of particles generated from various wt% of phenolic resins: (a) 0.06, (b) 0.125, (c) 0.25, (d) 0.5 and (e) 1.0.

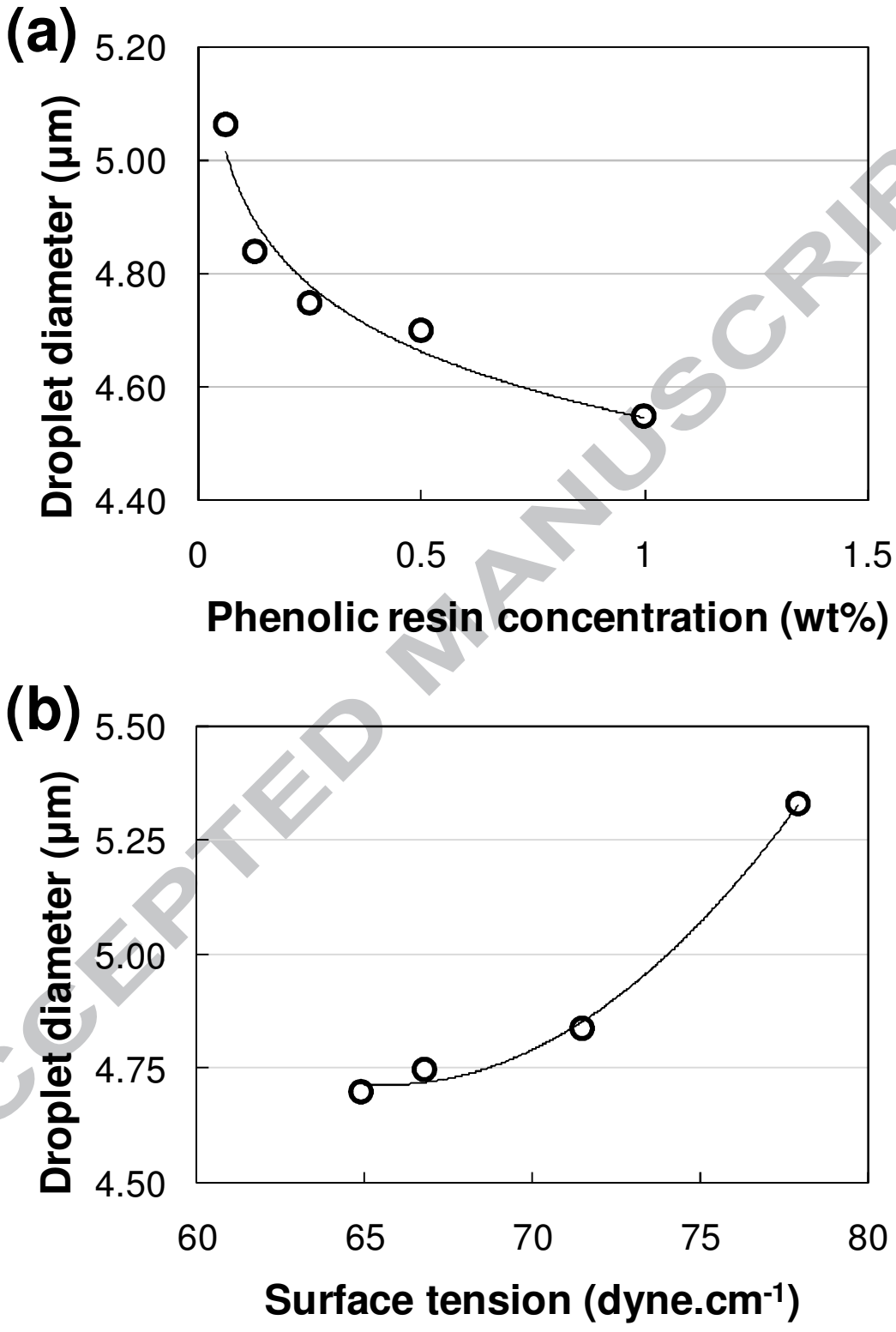

Figure 8. Effect on droplet diameter of (a) phenolic resin concentration and (b) surface tension.

3.2.2. Porous particles

In the case of porous carbon, Figure 9 shows that the particle enlarged when the PSL to phenolic resin ratio was increased from 0.8 to 1.6, but that little change was observed when the ratio was further increased to 3.2. The enlargement of the particles is proportional to the porosities, which were observed to be 0.21, 0.38, and 0.47 for PSL to phenolic resin mass ratio of 0.8, 1.6, and 3.2, respectively. Because the phenolic resin concentration was held constant, this may be explained by limited particle shrinkage during the earlier stage of carbonization where PSL particles should have started to decompose. The remaining PSL particles during the early stage may have acted as a barrier to shrinkage, which was then only driven by the phenolic resin. Significant shrinkage of the particle only then occurred when PSL particles had completely decomposed. At high PSL concentrations, this barrier to shrinkage becomes more dominant and results in insignificant changes to the overall particle size.

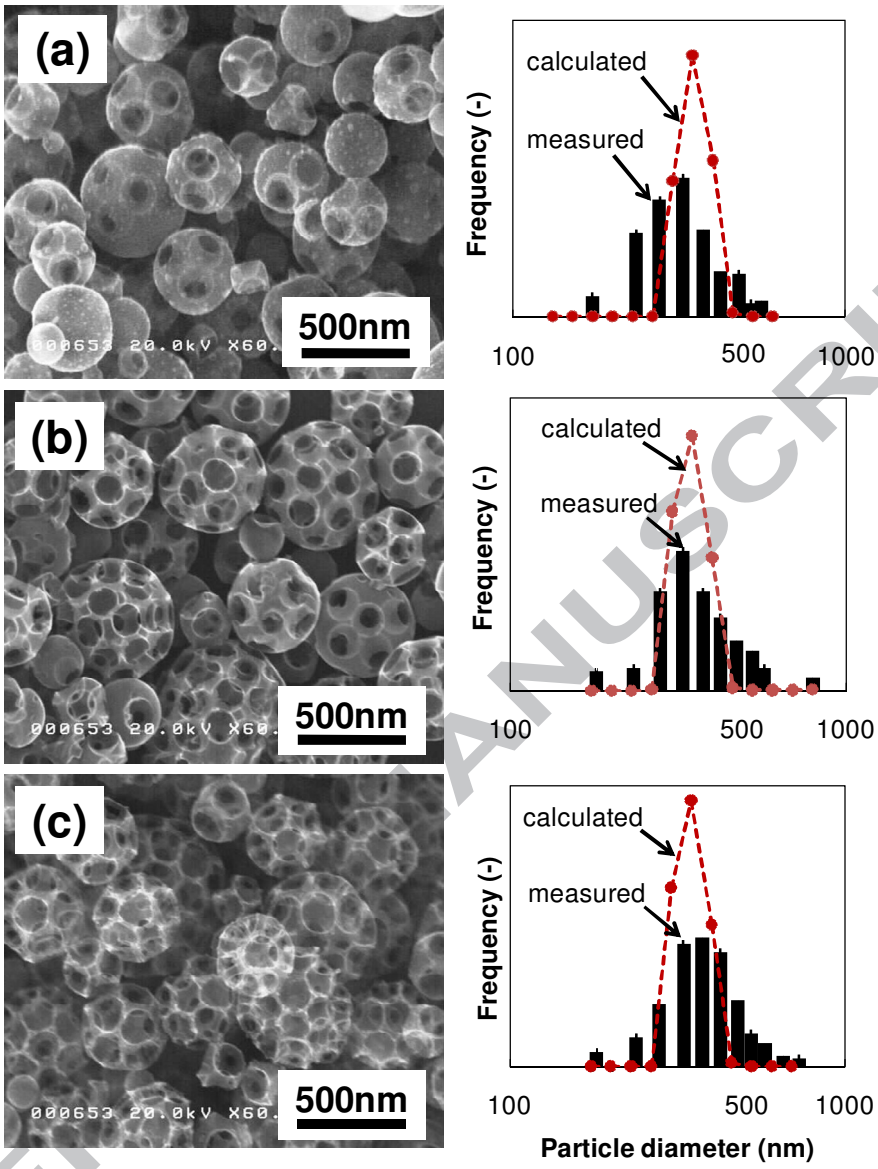

Figure 9. SEM images and size distributions of particles generated from PSL: phenolic resin concentrations of (a) 0.8, (b) 1.6, and (c) 3.2. For all cases, the phenolic resin concentration was 0.25 wt%.

3.3. Developing a correlation for dense particles

A number of factors were then considered in the development of the correlation to predict particle size. The dimension of a particle can be estimated if the mass and the mass density of the particle are known, but in spray pyrolysis the starting material decomposes into a number of decomposition products [21, 29]. Determining the conversion of a precursor is simpler if the stoichiometry of the decomposition is well understood, but this is not the case for the pyrolysis of phenolic resin. Jiang et al. [30] used a simulation approach to determine the number of gas

molecules released during the spray pyrolysis of phenolic resin. However, their simulation did not fully represent the complete pyrolysis process and the stoichiometry cannot be extracted from it.

Because a representative reaction model is not available, another approach to approximate the phenolic resin to carbon ratio by measuring the pyrolysis yield was carried out. Pyrolysis yield was obtained by measuring the mass of the obtained particles divided by the mass of consumed phenolic resin. The average yield of carbon from phenolic resin using spray pyrolysis in our experiments was 21.63% (mass basis) and remained constant at phenolic resin concentrations between 0 and 1 wt%. Assuming that the measured particles were obtained from a complete decomposition reaction, this value is hereafter referred to as the residual ratio (α), which is defined as the mass ratio between the yield and the main precursor component. The mass of the converted phenolic resin (X_{ph}) is explained by Equation (4) as follows:

$$X_{ph} = V_d \rho_d C_{ph} \alpha \tag{4}$$

where V_d is the droplet volume, ρ_d is droplet density, and C_{ph} is the concentration of the phenolic resin. According to the mass conservation law, the value of X_{ph} is equal to the mass of the final particle, hence:

$$V_d \rho_d C_{ph} \alpha = V_p \rho_c \tag{5}$$

where V_p and ρ_c are the particle volume and carbon mass density, respectively. Both the droplet and the particle are assumed to be perfectly spherical with a volume defined as $(4/3)\pi r^3$. Equation (5) then becomes:

$$\frac{4}{3}\pi\left(\frac{D_{d,v}}{2}\right)^3 \rho_d C_{ph} \alpha = \frac{4}{3}\pi\left(\frac{D_{p,v}}{2}\right)^3 \rho_c \tag{6}$$

While rearrangement of Equation (4) gives:

$$D_{p,v} = D_{d,v}\left(\frac{\alpha C_{ph} \rho_d}{\rho_c}\right)^{1/3} \tag{7}$$

Figure 10 (a) compares the mean particle diameters predicted by Equation (7) with experimental measurements. Equation (7) demonstrates a good fit to the experimental data, lying within the measurement standard deviation, and shows a significant improvement from Equation (1) (inset).

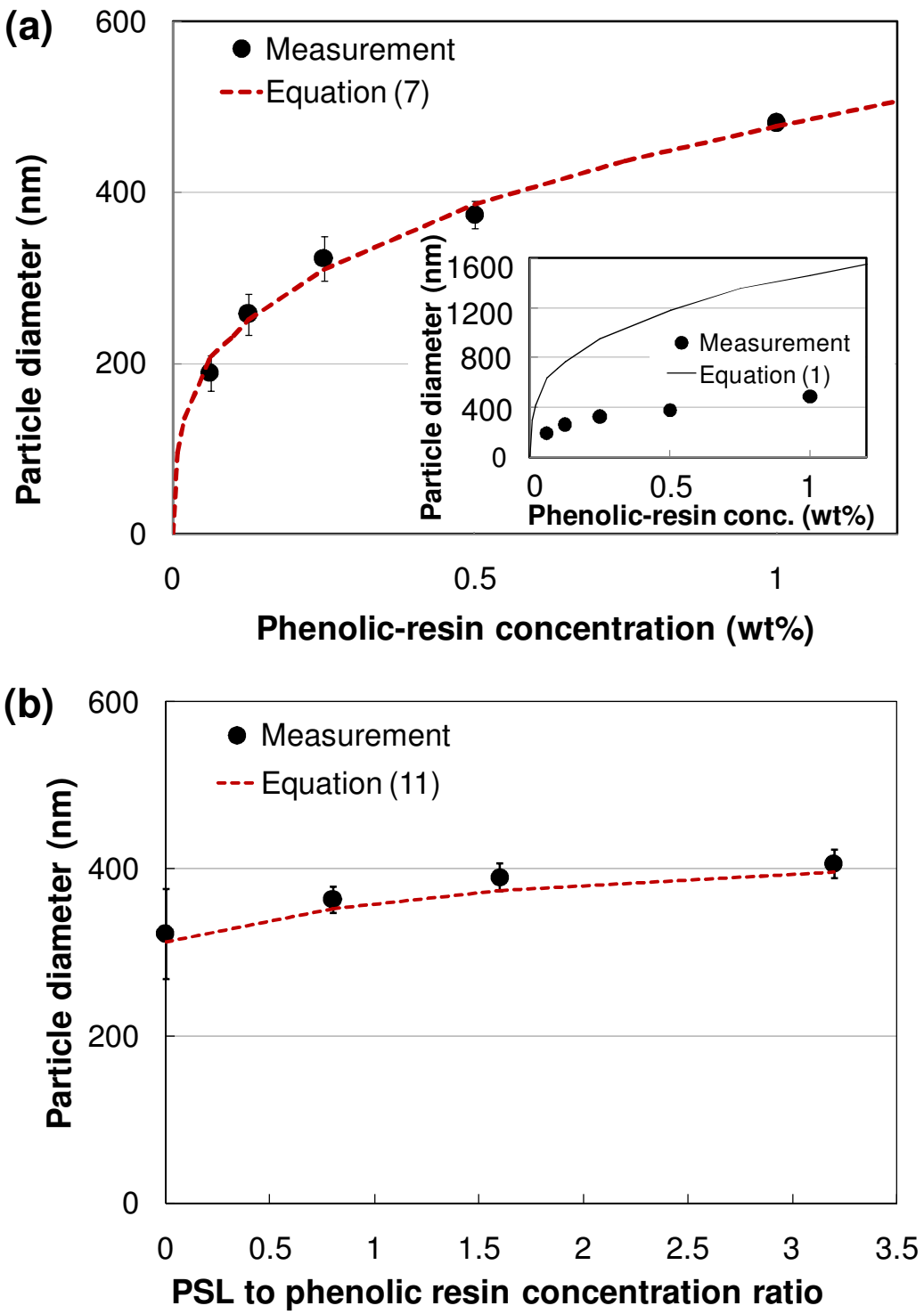

Figure 10. Comparison of experimental results with predicted mean diameters for (a) dense carbon particles using Equations (1) (inset) and (7), and (b) porous carbon particles using Equation (11).

Equation (7) was then used to predict final particle size distribution from the droplet size distribution data. The results shown in Figure 7 indicate that the predicted modal mean of the particle distribution largely coincides with that measured experimentally. However, the measured particle size distribution was wider than predicted by Equation (7). This suggests some of the particles failed to satisfy the one-droplet-one-particle formation principle with a small amount of droplets either segregating or aggregating. A detailed explanation of the formation mechanism merits further study, although a preliminary, speculative mechanism using a momentum balance is proposed here. Using the principle of the conservation of momentum, the velocity profile inside the tube was approximated by Equation (8).

$$\rho v_z\left(\frac{\partial v_z}{\partial z}\right)=\mu\left(\frac{1}{r}\frac{\partial}{\partial r}\left(r\frac{\partial v_z}{\partial r}\right)+\frac{\partial^2 v_z}{\partial z^2}\right)+\rho g_z \qquad (8)$$

The velocity profile of the fluid inside the tube (based on FlexPDE simulation results) is shown in Figure 11 where the velocity at the center of the tube was higher than at the edge. The difference in velocity causes the droplets at the center of the tube to be displaced faster than those at the edge resulting in inter-droplet friction. Such friction could either lead droplets to agglomerate or segregate, as illustrated in Figure 11.

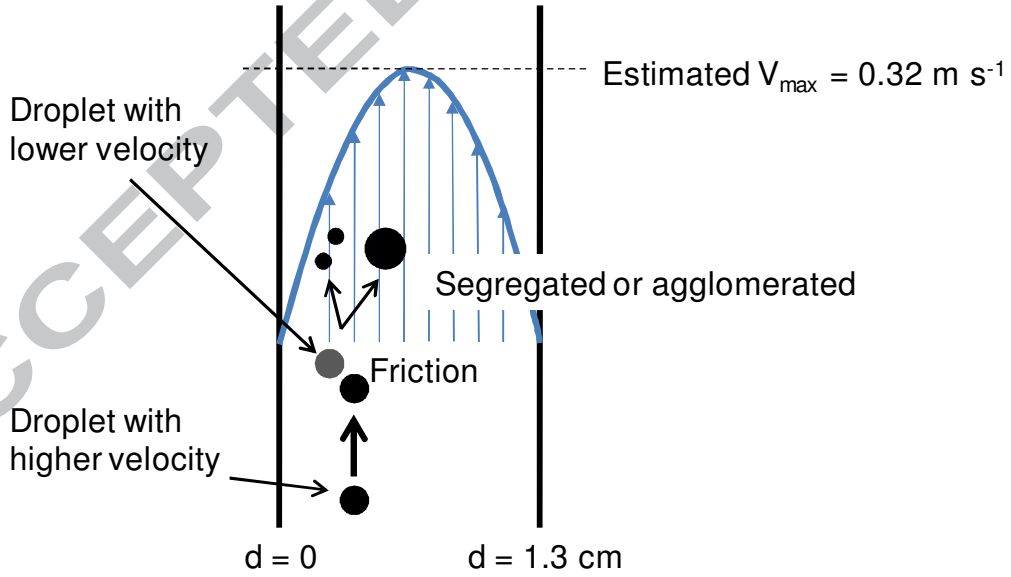

Figure 11. Schematic of velocity profile inside the tube at distance of 5 cm from the tube inlet illustrating the impact of friction between droplets with different velocities.

The difference between the predicted and measured particle size distribution, although small, suggests the possibility of producing particles with a relatively wide size distribution from droplets with narrow size distribution.

3.4. Developing a correlation for porous particles

While Equation (7) can successfully predict the size of dense carbon particles, further improvement is required for determining the size of porous particles. The addition of the template PSL created a number of pores in the particles. Although shrinkage of the particle still occurred following carbonization, the existence of the pores resulted in an increased size compared to the dense carbon particle. At higher PSL concentrations more pores were formed, further increasing the particle size. The number of pores is represented by the porosity (ε), which is defined as the ratio of pore to particle volume. Here, both α and ε are important in determining the final size of porous carbon particle.

Since porosity is defined as the ratio of pore to particle volume, the fraction of the solid phase in the particle will be equal to $(1-\varepsilon)$. According to the topological measurement, the solid fractions of carbon particles were 0.79, 0.62, and 0.53 for PSL to phenolic resin mass ratio of 0.8, 1.6, and 3.2, respectively. In developing the correlation, it is assumed that the solid phase in the porous particle is entirely carbon and that the mass of the phenolic resin that decomposes into carbon is equal to the mass of the solid phase of the particle. Therefore, the mass balance equation is rewritten as:

$$V_d \rho_d C_{ph} \alpha = V_p \rho_c (1-\varepsilon) \tag{9}$$

Modeling both the droplet and carbon particle as spheres yields:

$$\frac{4}{3}\pi\left(\frac{D_{d,v}}{2}\right)^3 \rho_d C_{ph} \alpha = \frac{4}{3}\pi\left(\frac{D_{p,v}}{2}\right)^3 \rho_c (1-\varepsilon) \tag{10}$$

which can then be rearranged to the form shown in Equation (11).

$$D_{p,v} = D_{d,v}\left(\frac{\alpha C_{ph} \rho_d}{\rho_c (1-\varepsilon)}\right)^{1/3} \tag{11}$$

Figure 10 (b) shows that Equation (11) can estimate the average particle size while the equation also shows good agreement with experimental data for the particle size distribution

(Figure 9). Similar reasons for slight deviations between experimental and modeled results exist for the same reasons as detailed for the dense particle case.

From the results here, a PSL to phenolic resin ratio of 3.2 is considered to be the maximum applicability limit of Equation (11) as well as the upper limit for synthesis of porous carbon particles as at higher ratios the particles tend to become brittle due to the very high porosity. As a result, a number of particles break apart and can no longer be treated as spherical. A further limiting factor is that the particle structure of PSL during self-assembly tended to be polygonal or polyhedral [31, 32]. Hence, at high PSL concentration the particle morphology would follow the structure of PSL again making spherical morphologies less common.

4. Conclusions

Correlations to predict the final particle size of dense carbon particles derived from phenolic resin and porous carbon particles derived from phenolic resin and a PSL template, synthesized via spray pyrolysis, have been developed. A residual ratio was introduced as a variable to represent the shrinkage during phenolic resin decomposition. In the porous carbon particle correlation, both residual ratio and porosity were considered in determining the particle size. Using the correlations to predict mean particle diameters showed good agreement with experimental results. The size of dense carbon particles was found to be strongly influenced by the concentration of the phenolic resin. Up to a limiting concentration, the addition of PSL also influenced the size of porous carbon particles. The predicted particle size distributions were narrower than experimental results, possibly due to the segregation and agglomeration of the droplets inside the tubular furnace, but particle size distribution was still well-predicted by the developed correlations.

Acknowledgements

This work was supported by JSPS KAKENHI Grant Number 22246099 and 26709061. The authors would like to thank Sumitomo Bakelite Co. Ltd. for supplying the phenolic resin and the Japanese Ministry of Education, Culture, Sports, Science and Technology (MEXT) for providing a doctoral scholarship (A.F.A.).

References

[1] K. Okuyama, I. Wuled Lenggoro, Preparation of nanoparticles via spray route, Chemical Engineering Science 58 (2003) 537-547.

[2] W.H. Suh, K.S. Suslick, Magnetic and porous nanospheres from ultrasonic spray pyrolysis, Journal of the American Chemical Society 127 (2005) 12007-12010.

[3] M. Eslamian, N. Ashgriz, Effect of precursor, ambient pressure, and temperature on the morphology, crystallinity, and decomposition of powders prepared by spray pyrolysis and drying, Powder technology 167 (2006) 149-159.

[4] R. Balgis, G. Anilkumar, S. Sago, T. Ogi, K. Okuyama, Rapid In Situ Synthesis of Spherical Microflower Pt/C Catalyst Via Spray-drying for High Performance Fuel Cell Application, Fuel Cells 12 (2012) 665-669.

[5] T. Ogi, A.B.D. Nandiyanto, K. Okuyama, Nanostructuring strategies in functional fine-particle synthesis towards resource and energy saving applications, Advanced Powder Technology 25 (2014) 3-17.

[6] R. Vehring, W.R. Foss, D. Lechuga-Ballesteros, Particle formation in spray drying, Journal of aerosol science 38 (2007) 728-746.

[7] S.Y. Lee, W. Widiyastuti, F. Iskandar, K. Okuyama, L. Gradoń, Morphology and particle size distribution controls of droplet-to-macroporous/hollow particles formation in spray drying process of colloidal mixtures precursor, Aerosol Science and Technology 43 (2009) 1184-1191.

[8] M. Vicent, E. Sánchez, T. Molina, M. Nieto, R. Moreno, Comparison of freeze drying and spray drying to obtain porous nanostructured granules from nanosized suspensions, Journal of the European Ceramic Society 32 (2012) 1019-1028.

[9] J. Elversson, A. Millqvist-Fureby, G. Alderborn, U. Elofsson, Droplet and particle size relationship and shell thickness of inhalable lactose particles during spray drying, Journal of pharmaceutical sciences 92 (2003) 900-910.

[10] R. Rajan, A. Pandit, Correlations to predict droplet size in ultrasonic atomisation, Ultrasonics 39 (2001) 235-255.

[11] M. Eslamian, N. Ashgriz, Spray drying, spray pyrolysis and spray freeze drying, Handbook of Atomization and Sprays, Springer2011, pp. 849-860.

[12] S. Jain, D.J. Skamser, T.T. Kodas, Morphology of single-component particles produced by spray pyrolysis, Aerosol Science and Technology 27 (1997) 575-590.

[13] S. Sharma, R. Kamath, M. Madou, Porous glassy carbon formed by rapid pyrolysis of phenol-formaldehyde resins and its performance as electrode material for electrochemical double layer capacitors, Journal of Analytical and Applied Pyrolysis 108 (2014) 12-18.

[14] H. Jiang, J. Wang, S. Wu, Z. Yuan, Z. Hu, R. Wu, Q. Liu, The pyrolysis mechanism of phenol formaldehyde resin, Polymer Degradation and Stability 97 (2012) 1527-1533.

[15] R. Balgis, T. Ogi, W.-N. Wang, G.M. Anilkumar, S. Sago, K. Okuyama, Aerosol Synthesis of Self-Organized Nanostructured Hollow and Porous Carbon Particles using a Dual Polymer System, Langmuir (2014).

[16] R. Balgis, T. Ogi, A.F. Arif, G.M. Anilkumar, T. Mori, K. Okuyama, Morphology control of hierarchical porous carbon particles from phenolic resin and polystyrene latex template via aerosol process, Carbon (2014).

[17] S. Xu, G. Qiao, H. Wang, D. Li, T. Lu, Preparation of mesoporous carbon derived from mixtures of phenol-formaldehyde resin and ethylene glycol, Materials Letters 62 (2008) 3716-3718.

[18] K. Lenghaus, G. GuangHua Qiao, D.H. Solomon, C. Gomez, F. Rodriguez-Reinoso, A. Sepulveda-Escribano, Controlling carbon microporosity: the structure of carbons obtained from different phenolic resin precursors, Carbon 40 (2002) 743-749.

[19] W.-N. Wang, A. Purwanto, I.W. Lenggoro, K. Okuyama, H. Chang, H.D. Jang, Investigation on the correlations between droplet and particle size distribution in ultrasonic spray pyrolysis, Industrial & Engineering Chemistry Research 47 (2008) 1650-1659.

[20] W.-N. Wang, W. Widiyastuti, I.W. Lenggoro, T.O. Kim, K. Okuyama, Photoluminescence optimization of luminescent nanocomposites fabricated by spray pyrolysis of a colloid-solution precursor, Journal of The Electrochemical Society 154 (2007) J121-J128.

[21] K.A. Trick, T.E. Saliba, Mechanisms of the pyrolysis of phenolic resin in a carbon/phenolic composite, Carbon 33 (1995) 1509-1515.

[22] H. Jiang, J. Wang, S. Wu, B. Wang, Z. Wang, Pyrolysis kinetics of phenol–formaldehyde resin by non-isothermal thermogravimetry, Carbon 48 (2010) 352-358.

[23] R. Balgis, S. Sago, G.M. Anilkumar, T. Ogi, K. Okuyama, Self-Organized Macroporous Carbon Structure Derived from Phenolic Resin via Spray Pyrolysis for High-Performance Electrocatalyst, ACS applied materials & interfaces 5 (2013) 11944-11950.

[24] S. Che, O. Sakurai, K. Shinozaki, N. Mizutani, Particle structure control through intraparticle reactions by spray pyrolysis, Journal of aerosol science 29 (1998) 271-278.

[25] I.W. Lenggoro, T. Hata, F. Iskandar, M.M. Lunden, K. Okuyama, An experimental and modeling investigation of particle production by spray pyrolysis using a laminar flow aerosol reactor, Journal of materials research 15 (2000) 733-743.

[26] Y. Xiong, T.T. Kodas, Droplet evaporation and solute precipitation during spray pyrolysis, Journal of aerosol science 24 (1993) 893-908.

[27] A. Gurav, T. Kodas, T. Pluym, Y. Xiong, Aerosol processing of materials, Aerosol Science and Technology 19 (1993) 411-452.

[28] R.J. Lang, Ultrasonic atomization of liquids, The journal of the acoustical society of America 34 (1962) 6-8.

[29] Y. Yamashita, K. Ōuchi, A study on carbonization of phenol-formaldehyde resin labelled with deuterium and< sup> 13</sup> C, Carbon 19 (1981) 89-94.

[30] D.-e. Jiang, A.C. Van Duin, W.A. Goddard III, S. Dai, Simulating the initial stage of phenolic resin carbonization via the ReaxFF reactive force field, The Journal of Physical Chemistry A 113 (2009) 6891-6894.

[31] M. Abkarian, A.B. Subramaniam, S.-H. Kim, R.J. Larsen, S.-M. Yang, H.A. Stone, Dissolution arrest and stability of particle-covered bubbles, Physical review letters 99 (2007) 188301.

[32] R. Aveyard, J.H. Clint, D. Nees, V.N. Paunov, Compression and structure of monolayers of charged latex particles at air/water and octane/water interfaces, Langmuir 16 (2000) 1969-1979.

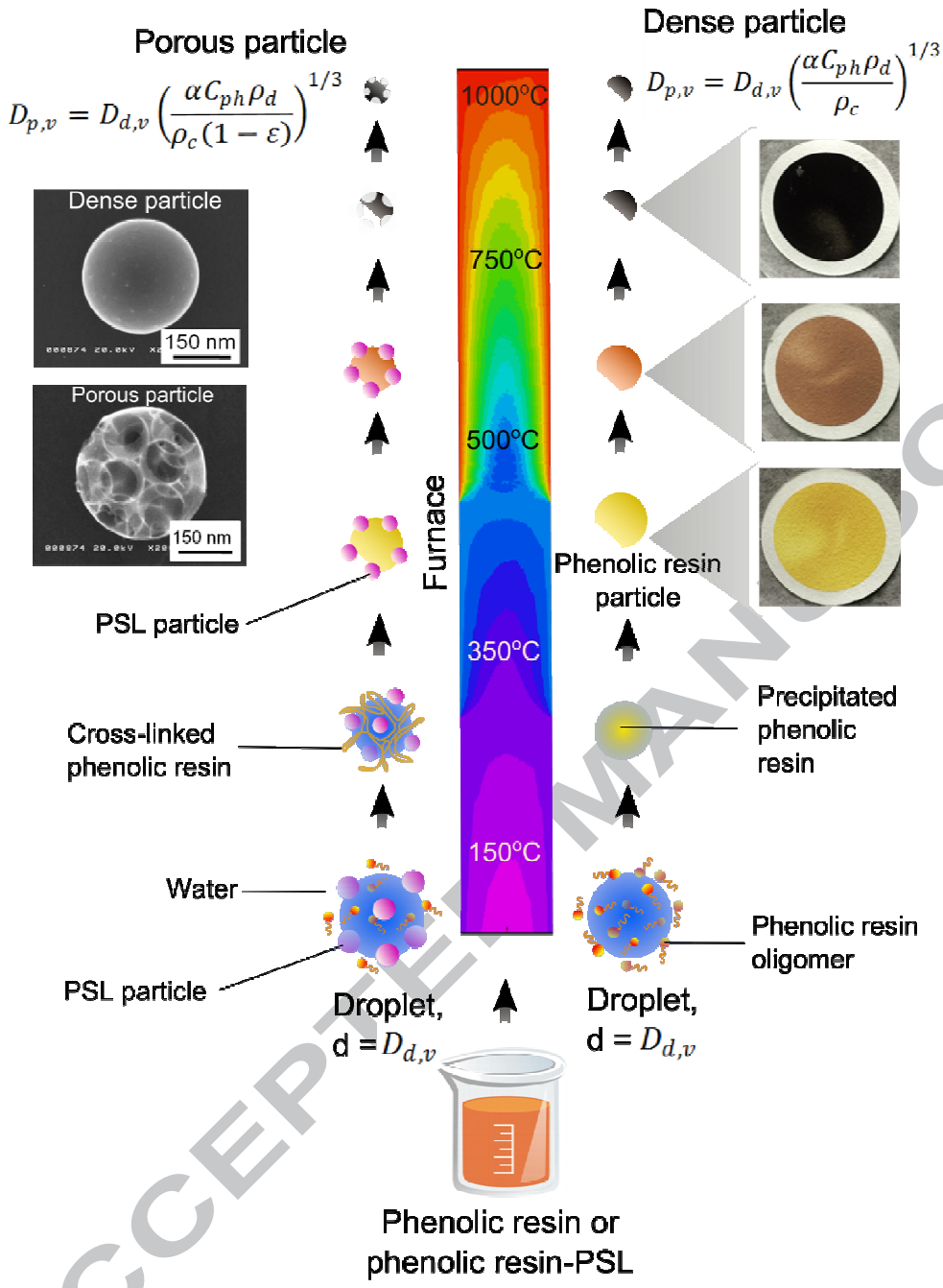

1

2

Highlights:

- Droplet diameter was measured using laser diffraction technique
- Pyrolysis conversion of phenolic resin to nanostructured carbon was evaluated
- New equation to predict carbon particle size was developed from mass balance
- Shrinkage of carbon particle is included in the proposed equation
- Particle diameters from proposed equations and measurement are in good agreement